Design of a double-pass shear mode acousto-optic modulator

Chih-Hao Chang,[1,a)] R. K. Heilmann,[1] M. L. Schattenburg,[1] and P. Glenn[2]
[1]*Space Nanotechnology Laboratory, Massachusetts Institute of Technology, Cambridge, Massachusetts 02139, USA*
[2]*Bauer Associates, Inc., 8 Tech Circle, Natick, Massachusetts 01760, USA*

(Received 26 November 2007; accepted 16 February 2008; published online 12 March 2008)

The design of a compact double-pass shear mode acousto-optic modulator for high power operation in the UV is presented. Using a spherical mirror retroreflector in the second pass to correct for beam deflection, changes in beam position and angle during frequency tuning can be eliminated. The use of the shear mode acousto-optic interaction offers several key advantages, but the strain-induced birefringence creates significant levels of spectral leakage in the system. These effects and the polarization of the beams are analyzed to minimize leakage. Using a heterodyne interferometry scheme, two double-pass acousto-optic modulators with offset acoustic frequency inputs are set up to measure the leakage intensity. The designed double-pass shear mode acousto-optic modulator was tested with $\lambda = 351.1$ nm and demonstrated a peak double-pass efficiency of 42.6% and a bandwidth of 28 MHz. Over this bandwidth the spectral leakage was reduced to $\sim 0.01\% - 0.04\%$ relative intensity. © *2008 American Institute of Physics.* [DOI: 10.1063/1.2894210]

I. INTRODUCTION

The acousto-optic interaction occurs when a light beam diffracts from a periodic perturbation in a material medium caused by an acoustic wave. Since the perturbation has a velocity vector, the diffracted beam is Doppler shifted by the frequency of the acoustic wave.[1] This phenomenon is useful for high speed frequency modulation of optical beams. There are various frequency shifting applications for acousto-optic modulators (AOMs), such as displacement measuring interferometry,[2,3] spectral tunable filters,[4] and *Q*-switching and mode locking in a laser cavity. For our application, we utilize AOMs for frequency shifting in a digital heterodyne fringe-locking system for interference lithography.[5,6]

A common problem with AOMs is that the beam diffraction angle changes with the input acoustic frequency. Such an effect can be eliminated by using the AOM in a double-pass configuration, as Donley *et al.*[7] presented using a longitudinal AOM designed for the visible to near-infrared range. In such a configuration the change in diffraction angle is compensated by the second pass, and the output beam of the system has no beam displacement effects when changing the acoustic frequency. However, the double-pass system contains multiple optical interfaces, and unwanted back-reflection or scattering may result in light with a frequency that is different from the desired one at the output. Such spectral leakage is not easily detectable by eye during alignment and can cause ill effects if ignored. For example, in interference lithography it creates nonstationary intensity patterns,
resulting in a constant background exposure of photoresist and reduction of fringe contrast.

For UV radiation, the shear mode AOM is more desirable due to its larger diffraction angle. This condition reduces the overall physical size of the system and is critical for a complex optical system. However, designing a double-pass configuration in shear mode poses several challenges, the most significant one being the polarization effects of the shear mode acousto-optic interaction and its effect on the spectral leakage of the system. This paper presents a compact and versatile design of a double-pass shear mode AOM for high power UV light sources. A heterodyne interferometric setup was used to determine and reduce the level of spectral leakage in the double-pass system.

II. POLARIZATION EFFECTS IN SHEAR MODE ACOUSTO-OPTIC INTERACTION

There are two modes of acoustic waves that can be used in an acousto-optic interaction—the longitudinal and the shear mode. Both modes offer their own advantages, and selection is based on the application. One advantage for the shear mode is that in a solid medium the velocity of a shear wave is typically slower, resulting in a perturbation that has a shorter period. For Bragg regime acousto-optic diffraction in the small angle approximation, the Bragg angle within the crystal is given by

$$\theta_B = \frac{f_{\mathrm{rf}}\lambda}{2nv}, \tag{1}$$

where f_{rf} is the acoustic frequency, λ is the optical wavelength, n is the index of refraction of the solid medium, and v is the velocity of the acoustic wave. The separation angle, which is the angle between the zeroth and the diffracted first orders exiting the crystal, is then approximately twice the product of the Bragg angle and the material index. Due to the lower acoustic wave velocity, Eq. (1) shows that the Bragg angle for a shear mode AOM is larger, ensuring a larger separation of the diffracted orders. This is especially critical for beams with shorter wavelength. For our lithography sys-

a)Electronic mail: chichang@mit.edu.

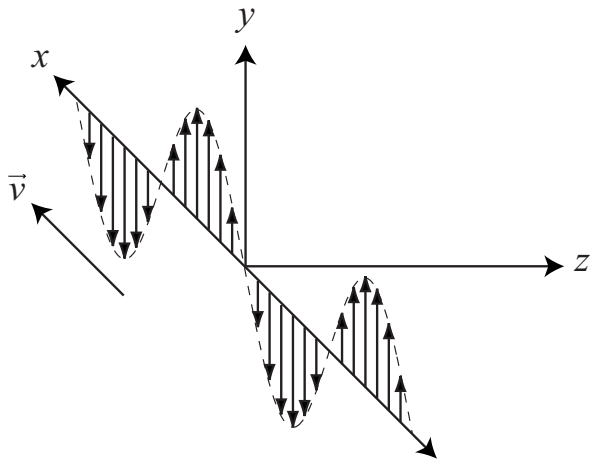

FIG. 1. Coordinate frame for shear mode acousto-optic interaction, depicting a shear-mode acoustic wave propagating along the x axis with particle motion along the y axis.

tem where a UV source of 351.1 nm wavelength is used, fused silica is one of the few materials that is transparent at this wavelength. Acoustic shear and longitudinal waves travel at 3761 and 5960 m/s in fused silica,[1] respectively. For 100 MHz acoustic input, a shear mode AOM has a separation angle of 9.34 mrad, significantly greater than 6.18 mrad for operation in the longitudinal mode.

Although a shear mode AOM has larger diffraction angles, a major disadvantage is its effect on light polarization.[1,8] To minimize the effects of leakage in the AOM, the polarization effects need to be analyzed and taken into account. For an acoustic shear wave propagating in the x-direction and polarized with particle motion in the y-direction, as shown in Fig. 1, the strain field in reduced indices is given by

$$S_6 = S\sin(\Omega t - Kx), \tag{2}$$

where S is the strain amplitude, Ω is the frequency, and K is the wave vector of the acoustic wave. The linear photoelastic effect can be described by the tensor equation[1]

$$\Delta\eta_{ij} = p_{ijkl}S_{kl}, \tag{3}$$

where $\Delta\eta_{ij}$ and S_{kl} are the second-rank impermeability and strain tensors, respectively, and p_{ijkl} is the fourth-rank strain-optic tensor. Using the strain-optic coefficients for fused silica, the optical impermeability tensor for a shear wave is given by

$$\Delta\eta_{ij} = \begin{pmatrix} 0 & (1/2)S_6(p_{11}-p_{12}) & 0 \\ (1/2)S_6(p_{11}-p_{12}) & 0 & 0 \\ 0 & 0 & 0 \end{pmatrix}, \tag{4}$$

where p_{11} and p_{12} are the only independent coefficients for an isotropic material such as fused silica. Since the nonzero terms in Eq. (4) represent shear terms, there will be an x-y cross term in the index ellipsoid equation. To eliminate the cross term, the x and y principal axes are rotated 45° about the z axis. The equation for the rotated ellipsoid thus becomes

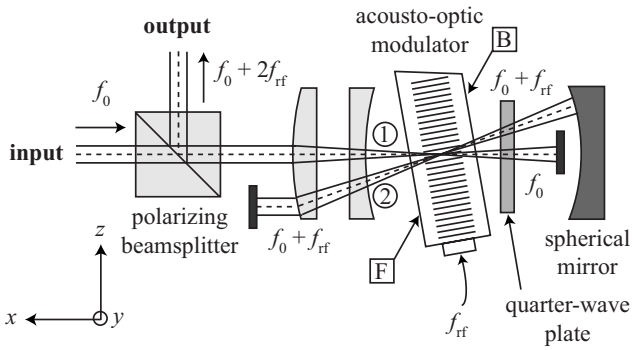

FIG. 2. Optical configuration for the shear mode double-pass AOM.

$$x'^2\left[\frac{1}{n^2} + \frac{1}{2}S_6(p_{11}-p_{12})\right] + y'^2\left[\frac{1}{n^2} - \frac{1}{2}S_6(p_{11}-p_{12})\right] + \frac{z^2}{n^2} = 1, \tag{5}$$

and the refractive indices for the rotated principal axes x' and y' are

$$n_{x'} = n - \tfrac{1}{4}n^3S(p_{11}-p_{12})\sin(\Omega t - Kx),$$

$$n_{y'} = n + \tfrac{1}{4}n^3S(p_{11}-p_{12})\sin(\Omega t - Kx). \tag{6}$$

The sign difference between the x' and y' axes in Eq. (6) ensures that the sinusoidal perturbations in these two directions are always out of phase by π. Thus for light propagating along the z-direction, the shear mode AOM behaves like a half-wave plate with its optical axis oriented 45° to the x-direction for the Bragg diffracted beam.[9,10] This polarization effect is not present in the longitudinal mode acousto-optic interaction, and it plays an important role in analyzing the spectral leakage in the double-pass AOM.

III. DOUBLE-PASS CONFIGURATION

After analyzing the polarization effects of the shear mode acousto-optic diffraction, a double-pass configuration can be designed to eliminate the beam displacements due to changing frequency. Figure 2 depicts the optical setup for the shear mode double-pass AOM (note the different reference frame being used). Setting the x-z plane as the plane of incidence, a TM-polarized beam is transmitted by a polarizing beamsplitter cube and focused onto the AOM crystal (Neos Technologies,[11] model 46100). The diffracted first order, Doppler shifted by f_{rf}, is now TE polarized due to the shear mode acousto-optic effect. It then goes through a quarter-wave plate twice while being focused back onto the AOM crystal by a spherical mirror, effectively changing the beam back to TM polarization. The AOM diffracts the beam for the second pass, while rotating its polarization to TE and Doppler shifting it by f_{rf}. The beam, now having a frequency of f_0+2f_{rf}, propagates back toward the polarizing beamsplitter and is reflected as the output beam. The unwanted orders are blocked by beam blocks in the setup.

The focusing lenses, separated by 61.7 mm, are plano-convex and planoconcave with foci of 81.1 and −21.6 mm, respectively. They are used to focus the 1 mm diameter

$(1/e^2)$ beam onto the AOM 37.3 mm away. The AOM crystal material is fused silica, and the operating acoustic frequency is centered around 100 MHz, resulting in a separation angle of 9.34 mrad. A focused Gaussian beam is used in the AOM because the shear transducer creates a relatively small effective acoustic aperture of 200 μm. The strain field is also not uniform, resulting in diffraction efficiency that is position sensitive. This can be problematic if the beam angle at the input is not stable, as the lens will translate beam angle variations into lateral shifts on the AOM crystal and cause the efficiency to fluctuate with time.

Focusing inside the crystal is also more desirable than other schemes, such as a cat's eye retroreflector,[7] since fused silica has a high optical power threshold. Focusing UV radiation on mirrors might build up organic contamination on the reflective coating. Instead, a spherical mirror with radius of 150 mm is used to focus the diverging beam back onto the AOM. The spherical mirror is placed so that the wavefront curvature matches the mirror curvature, effectively retroreflecting the beam. This position can be determined readily by propagating the complex beam parameter using the ABCD ray transfer matrix.[1] The initial beam parameter $q_0 = jz_0$ is defined at the beam waist inside the AOM crystal, where $z_0 = \pi\omega_0^2/\lambda$ and ω_0 is the radius of the beam waist. The beam then propagates a distance t in fused silica, a fused silica/air interface, and distance z in air. The transferred beam parameter as a function of z is then

$$q(z) = \frac{q_0 + t}{n} + z, \tag{7}$$

where n is the refractive index of fused silica. The wavefront radius can then be determined from

$$R(z) = \left(\frac{t}{n} + z\right)\left[1 + \frac{z_0^2}{(t + nz)^2}\right]. \tag{8}$$

Using system parameters $\omega_0 = 65$ μm and $t = 5$ mm, the wavefront curvature matches the spherical mirror at $z = 142.1$ mm. It is important to note that this condition is satisfied exactly only at a particular acoustic frequency. When changing operating frequency, the shift in diffraction angle changes the optical path. However, within the full width at half maximum (FWHM) bandwidth of our system the angular shifts are less than ~ 1 μrad, and the effects are negligible.

The AOM is driven by 6 W of acoustic power, with the double-pass efficiency as a function of input frequency shown in Fig. 3. The figure shows a double-pass peak efficiency of 42.6% at 105 MHz and a FWHM bandwidth of $\sim$28 MHz. The peak double-pass efficiency is comparable to the square of the measured maximum single-pass efficiency of $\sim$67%. The output beam was measured by a complementary metal oxide semiconductor (CMOS) camera (Cohu,[12] model 7200) to have less than 20 μm lateral and 10 μrad angular beam displacements within the FWHM bandwidth.

IV. SPECTRAL LEAKAGE

The double-pass AOM configuration eliminates the issue of beam displacement with changing acoustic frequency.

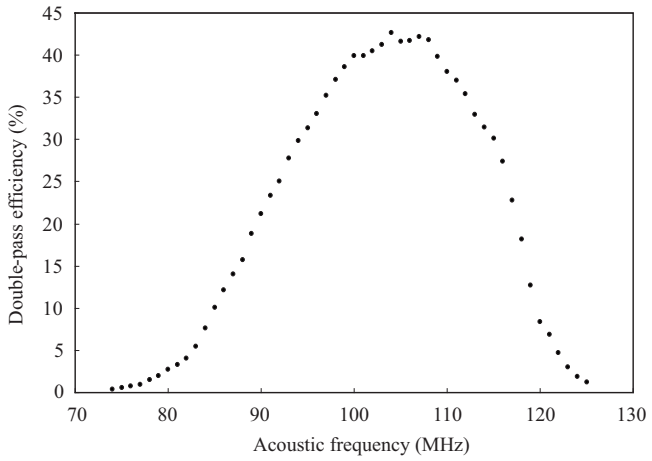

FIG. 3. Measured diffraction efficiency of the shear mode double-pass acousto-optic modulator.

However, the multiple optical components make the system prone to spectral leakage, even if perfectly aligned. The leakage originates from backreflections of the optical interfaces which have a reflectivity of $\sim$1% with antireflection coatings. The polarizing beamsplitter, as shown in Fig. 2, acts like a polarizer and only reflects $\sim$1% of TM-polarized output light. It is then desirable that the unwanted reflections are TM polarized to minimize spectral leakage in the output.

To evaluate the effects of leakage, the spectral components of the beam at the output of the double-pass AOM setup are examined. The reference frame in Fig. 2 is being used in this analysis. Assuming only frequency shifts caused by the acousto-optic effect, and that the beam is a TE-polarized plane wave propagating in the z-direction, the electric field can be written as the sum of spectral components,

$$E_y(z,t) = \sum_m A_m \exp[-j2\pi(f_0 + mf_{\mathrm{rf}})t + jkz]$$
$$= \sum_m g_m(f_0 + mf_{\mathrm{rf}}), \tag{9}$$

where k is the wave vector, A_m are the amplitudes for each spectral component, and m is an integer number representing the number of times the beam undergoes acousto-optic interaction. The intensity of the mth spectral component is thus $|A_m|^2$, and the double-pass signal component is described by $m = 2$. For convenience, Eq. (9) can be expressed as a sum of frequency components $g_m(f_0 + mf_{\mathrm{rf}})$. The output beams, having different frequencies, will beat and form a heterodyne intensity signal that contains the frequency differences of the components. The heterodyne signal can then be measured by a photodetector to examine the level of leakage. However, using this method the heterodyne frequencies will always be multiples of f_{rf}, and it will be difficult to determine the absolute frequency of each leakage component. Another consideration is that the operating acoustic frequency f_{rf} is around 100 MHz, and expensive electronics with high speed A/D will be required.

In order to analyze the spectral leakage more accurately, a setup with two double-pass AOMs operating at offset acoustic frequencies was used, as illustrated in Fig. 4. A

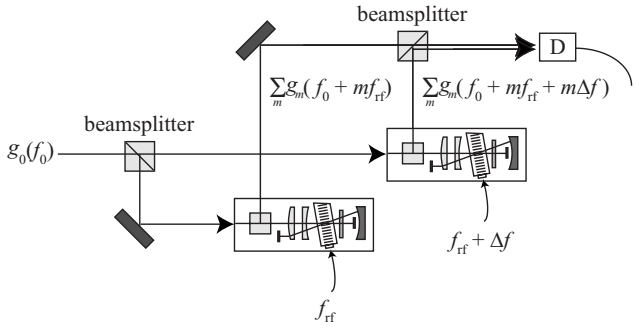

FIG. 4. Experimental setup to measure the magnitude of spectral leakage components.

beam with optical frequency f_0 is split into two by a beamsplitter cube, each beam entering a double-pass AOM setup. The input acoustic frequencies for the two AOMs are f_{rf} and $f_{rf}+\Delta f$, where Δf is a constant frequency offset chosen in the kilohertz range. The outputs of the double-pass AOMs are combined by a second beamsplitter and then measured by a photodetector. Due to the frequency offset Δf, the heterodyne signal contains high frequencies in the hundreds of megahertz range and low frequencies in the kilohertz range. The higher frequencies are blocked by a low-pass filter, while the lower frequencies can be analyzed by a spectrum analyzer (Hewlett-Packard model 35670A). The filtered heterodyne intensity signal in this setup is then given by

$$I(t) = I_0 + \sum_m |A_m|^2 \cos(2\pi m \Delta f t), \tag{10}$$

where I_0 is the background dc intensity. Equation (10) shows that by using this technique, the mth spectral component is represented as having a frequency of $m\Delta f$ and can be measured independently. An important assumption in this formulation is that the spectral leakage characteristics in the two double-pass AOM setups are the same. While this condition cannot be exact, the assumption is reasonable since the two setups differ only by alignment tolerances and have comparable performance to within a few percent. Using this experimental setup, the relative intensity of each spectral component in the double-pass AOM setup can be measured.

For an acoustic frequency input f_{rf} of 105 MHz and Δf of 20 kHz, the measured spectrum of the heterodyne intensity signal is plotted in Fig. 5(a). The figure illustrates the desired double-pass signal at 40 kHz and a single-pass leakage component at 20 kHz with ~0.02% relative intensity. Higher orders have insignificant intensity and are ignored in further analysis. The broad bandwidth close to dc and around the signal frequency are due to the lack of vibration isolation in the experimental setup. Using Eq. (9), the intensity $I=|E_y(z,t)|^2$ is

$$I(t) = |A_1|^2 + |A_2|^2 + 2A_1A_2 \cos(2\pi f_{rf} t), \tag{11}$$

where A_1 and A_2 are the amplitudes of the single-pass leakage and double-pass signal, respectively. Using $|A_1|^2 \sim 0.002|A_2|^2$ as measured, the leakage will interfere with the signal beam and result in $2A_1A_2/(A_1^2+A_2^2) \sim 9\%$ relative intensity fluctuations at a frequency of f_{rf}. In order to enable better dose and process control in lithography, this leakage-induced fluctuation needs to be reduced to a few percent.

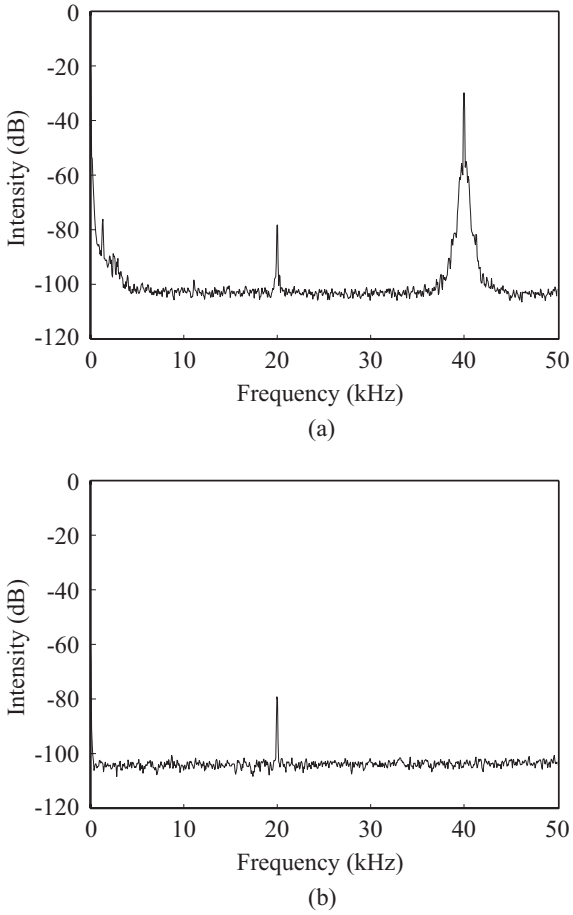

FIG. 5. Semilogarithmic plot of measured intensity spectra with nominal acoustic frequency input of 105 MHz and Δf of 20 kHz for (a) a double-pass AOM and (b) with the beam paths after the AOMs blocked. The band around dc, caused mostly by vibration of the signal beam, is much reduced as the beam paths are blocked.

To trace the sources of the single-pass leakage, another set of data, shown in Fig. 5(b), was taken with the beam paths after the AOM blocked in both setups. The leakage remained, suggesting that the majority of leakage is not coming from the optics after the AOM. The leakage is then determined to predominately originate from the back AOM/air interface, shown in Fig. 2 as surface "B." Due to the shear acousto-optic effect, the diffracted beam after the first-pass through the AOM is TE polarized. It then backreflects from the back AOM/air interface (along path 1 in Fig. 2) and results as leakage at the output. While this beam path is a significant source of leakage, it is not the only source; other weaker sources may exist in the system. Note that while this beam may be partially diffracted a second time by the acoustic wave after reflection, any doubly diffracted orders will be TM polarized and spatially separated to be blocked by the beam blocks (along path 2 in Fig. 2).

Since this leakage beam does not go through a second pass to compensate for the diffraction angle, it moves at the output when the acoustic frequency is changed. This can be observed by the CMOS camera with a long integration time. Due to this characteristic, the single-pass leakage beam is displaced from the signal beam at the output for a certain

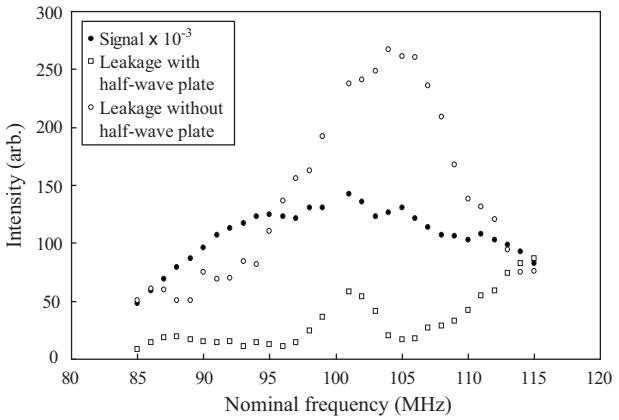

FIG. 6. Relative intensity of the double-pass signal and single-pass leakage components over the FWHM band of the double-pass AOM. The signal intensity is scaled by 10^{-3}.

frequency range. In this case, the leakage can be easily eliminated by using spatial filters. However, since the leakage sweeps in angle with frequency, it is difficult to filter out at all operating frequencies. It is important that the overall leakage intensity be reduced.

To reduce the single-pass leakage, a half-wave plate with its optical axis oriented at 22.5° to the z axis in Fig. 2 was placed after the polarizing beamsplitter. The quarter-wave plate after the AOM is also rotated by 45°. The purpose of the half-wave plate is to rotate the incoming TM-polarized beam by 45°, aligning it to the principal optical axis of the shear mode AOM. The beam then does not undergo any polarization effects in the AOM, and the polarization of the back AOM/air reflection will be rotated back to TM. As a result, the single-pass leakage is transmitted through the polarizing beamsplitter.

To verify the effects of the half-wave plate over the FWHM bandwidth of the double-pass AOM, the heterodyne experiment was repeated with nominal acoustic frequency inputs of 85–115 MHz and a constant Δf of 20 kHz. The results are plotted in Fig. 6. In this figure the magnitudes of the 40 kHz double-pass signal and the 20 kHz single-pass leakage components are plotted as functions of the nominal frequency. The signal magnitude is scaled by a factor of 10^{-3}. The spectral leakage is reduced to $\sim 0.01\% - 0.04\%$ relative intensity over the FWHM bandwidth. The reduction of spectral leakage is apparent, improving by a factor of up to ~20 at a nominal frequency of 105 MHz. Note that while the leakage from a single dominant source is reduced by the addition of the half-wave plate, leakage from other weaker undetermined sources remains. This is evident at the edge of the FWHM band around 115 MHz, where the half-wave plate had a negligible effect on presumably another leakage source. The residual leakage level is calculated to induce 2%–4% intensity fluctuations on the signal beam.

V. CONCLUSION

A double-pass AOM in shear mode designed for high power operation in the UV is presented. Such an optical system eliminates variations in beam position and angle during frequency tuning. Spectral leakage plays a critical role in shear mode acousto-optic interaction and is analyzed using an experimental setup with two double-pass AOMs actuated by offset acoustic frequencies. The leakage was found to be predominant from a single source and can be reduced by rotating the polarization of the incident beam. Tested with $\lambda = 351.1$ nm, the shear mode double-pass AOM demonstrated a peak efficiency of 42.6% with relative leakage intensity of $\sim 0.01\% - 0.04\%$ over the FWHM bandwidth of 28 MHz.

ACKNOWLEDGMENTS

We gratefully acknowledge the outstanding technical assistance of Robert Fleming and Jim Daley. Student, staff, and facility support from the Space Nanotechnology Laboratory, NanoStructures Laboratory, Quantum Nanostructures and Nanofabrication Group, and Microsystems Technology Laboratory at MIT are also appreciated. This work was supported by NASA Grant No. NNG05WC13G.

[1] A. Yariv and P. Yeh, *Optical Waves in Crystals* (Wiley, New York, 1984).
[2] N. Bobroff, Meas. Sci. Technol. **4**, 907 (1993).
[3] F. C. Demarest, Meas. Sci. Technol. **9**, 1024 (1998).
[4] S. E. Harris, S. T. K. Nieh, and D. K. Winslow, Appl. Phys. Lett. **15**, 325 (1969).
[5] R. K. Heilmann, P. T. Konkola, C. G. Chen, G. S. Pati, and M. L. Schattenburg, J. Vac. Sci. Technol. B **19**, 2342 (2001).
[6] C. G. Chen, P. T. Konkola, R. K. Heilmann, G. S. Pati, and M. L. Schattenburg, J. Vac. Sci. Technol. B **19**, 2335 (2001).
[7] E. A. Donley, T. P. Heavner, F. Levi, M. O. Tataw, and S. R. Jefferts, Rev. Sci. Instrum. **76**, 063112 (2005).
[8] A. Korpel, *Acousto-optics* (Dekker, New York, 1997).
[9] V. I. Balakshy and J. A. Hassan, Opt. Eng. (Bellingham) **32**, 746 (1993).
[10] A. Alippi, Opt. Commun. **8**, 397 (1973).
[11] http://www.neostech. com.
[12] http://www.cohu-cameras. com.